Mixing Enhancement in 3D MHD Channel Flow by Boundary Electrical Potential Actuation

Lixiang Luo and Eugenio Schuster

Abstract— **An electrically conductive fluid flowing inside a channel is prone to be affected by enormous magnetohydrodynamics (MHD) effects when the fluid interacts with an imposed magnetic field. Such effects often leads to higher pressure drop and lower heat transfer rate due to laminarization. Active boundary control, in either open loop or closed loop, can be used to enhance mixing and potentially increase heat transfer rate. Open-loop controllers are in general more sensitive to uncertainties of the system, which may result in a poorer performance. A closed-loop controller is proposed based on the linearized simplified magnetohydronamic (LSMHD) model. Micro pressure sensors and electrodes are embedded into the walls for measurement and actuation. Using the boundary vorticity flux as the input, the proposed feedback controller regulates the boundary electric potential at the channel walls in order to increase turbulence and mixing. By reversing the sign of a feedback controller designed to stabilize the LSMHD systems, a destabilizing controllers is achieved and used to excite multiple Fourier modes in simulations. The simulation results provided by a 3D simplified magnetohydronamic (SMHD) simulator show that the reversed controller successfully increases the turbulence inside an otherwise strongly stable MHD flow.**

I. Introduction

Magnetohydrodynamic (MHD) problems arise in many applications. One of them is cooling systems, where a liquid metal is often used as a heat transfer media. Because of their high thermal conductivity and high boiling point, liquid metals are highly favorable for applications with extreme conditions such as a fusion reactor cooling blanket. In this application certain liquid metals may also serve as fuel breeders as they react with the neutrons generated by the fusion reactions. In a fusion reactor a strong magnetic field is used to confine the plasma where the fusion reaction takes place; and this magnetic field inevitably affects the electrically conductive fluid in the cooling blanket. When the electrically conductive fluid flows in the presence of a transverse magnetic field, it generates an electric field due to charge separation and a subsequent electric current. The interaction between the induced current and the imposed magnetic field generates a body force, called the Lorentz force, which acts on the fluid itself. As the force acts in the opposite direction of the flow, it is necessary to increase the flow pressure gradient in order to maintain the average velocity of the flow and more power is needed to pump the liquid through the channel. In addition, the MHD effects tend to suppress perturbations and to laminarize the flow, reducing heat transfer rate as a consequence. A good review of the current status in this area can be found in [1].

Active control of fluid systems, implemented through micro electro-mechanical (MEM) or electro-magnetic actuators and sensors, can be used to achieve optimally the desired level of stability (when suppression of turbulence is desired) or instability (when enhancement of mixing is desired). The benefits of managing and controlling unsteady flows in engineering applications can be significant. This area has attracted much interest and has dramatically advanced in recent years [2], [3], [4], [5]. The boundary control of MHD flows has been considered for decades [6], [7], [8], [9], [10]. Research subjects range from strongly coupled MHD problems, like liquid metal and melted salt flows, to weakly coupled MHD problems, like salt water flows. Early research mostly focused on passive and open loop control. This situation is partly due to the complexity of the coupled MHD equations.

Our prior work includes several feedback control schemes for mixing enhancement in 2D MHD channel flows based on mechanical actuation at the boundary via blowing and suction. Micro-jets, pressure sensors, and magnetic field sensors embedded into the walls of the flow domain were considered in [11] to find a feedback control law that is optimal with respect to a cost functional related to a mixing measure. The effectiveness of the proposed controller for mixing and heat transfer enhancement has been illustrated in [12]. Another closed-loop controller was proposed in [13] based on a fixed-structure control law optimally tuned by extremum seeking. The moving speed of the fixed-structure traveling-wave-like boundary control was optimized in order to maximize a cost function defined as the heat transfer rate at the channel outlet. The numerical simulations confirmed that both closed-loop control schemes are effective in enhancing mixing and heat transfer by introducing 2D turbulence.

In this work we move to the problem of mixing enhancement in 3D MHD channel flows where only electromagnetic actuation is employed. We follow a linearization approach to develop a feedback controller based on the simplified MHD (SMHD) model. Spectral transformations are employed to transform the PDE system into a series of one-dimensional ODE systems. A feedback control law is designed to stabilize one of the ODE systems. The sign of the resulting controller is then reversed, which results into a linearly unstable feedback loop. By imposing a saturation limit for the controller, we successfully bound the instability and maintain a high level of turbulence near the walls. Simulation results are provided to illustrate the effectiveness of the controller.

This work was supported by the NSF CAREER award program (ECCS–0645086).

Lixiang Luo and Eugenio Schuster are with the Department of Mechanical Engineering and Mechanics, Lehigh University, Bethlehem, PA 18015, USA (lixiang.luo@lehigh.edu, schuster@lehigh.edu)

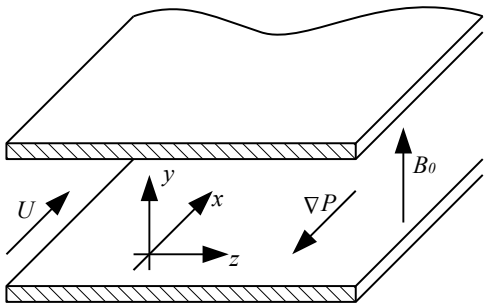

Fig. 1. System geometry

This article is organized as follows. In Section II, we state the system equations for incompressible SMHD flows, and derive the linearized version required for control synthesis. In Section III, the controller for the LSMHD system is designed, and the sign reversing procedure is discussed. In Section IV, simulation results are given in a typical magnetohydrodynamic physical setting. Section V closes the paper stating the conclusion and the identified future work.

II. Problem Statement

We consider a 3D, incompressible, electrically conducting fluid flowing between two parallel plates ($0<x<d=2\pi$, $0<z<\pi$ and $0<y<1$) along the x-direction, as illustrated in Fig. 1, where an external magnetic field B_0 is imposed perpendicularly to the plates, i.e., in the wall-normal y direction. This flow was first investigated experimentally and theoretically by Hartmann [14]. The mass flux Q is fixed. A uniform pressure gradient P_x in the x-direction is required to balance the boundary drag force and the body force due to the MHD effects. Space variables x, y, z, time t, velocity $\mathbf{v}$ and magnetic induction $\mathbf{B}$ are converted to their dimensionless forms:

$$x=\frac{x^*}{L},\qquad y=\frac{y^*}{L},\qquad z=\frac{z^*}{L},$$
$$\mathbf{B}=\frac{\mathbf{B}^*}{B_0},\qquad \mathbf{v}=\frac{\mathbf{v}^*}{U_0},\qquad j=\frac{\mathbf{j}^*}{U_0B_0},\qquad t=\frac{t^*U_0}{L},$$

where L, U_0 and B_0 are dimensional reference length, velocity and magnetic field. Variables denoted by the star notation are dimensional quantities.

The vector variables are defined as

$$\mathbf{v}(x,y,t)=u(x,y,t)\hat{\mathbf{x}}+v(x,y,t)\hat{\mathbf{y}}+w(x,y,t)\hat{\mathbf{z}},$$
$$\mathbf{B}(x,y,t)=B^u(x,y,t)\hat{\mathbf{x}}+B^v(x,y,t)\hat{\mathbf{y}}+B^w(x,y,t)\hat{\mathbf{z}},$$

where $\hat{\mathbf{x}}$, $\hat{\mathbf{y}}$ and $\hat{\mathbf{z}}$ are unit vectors in the x, y and z directions, respectively. The dimensionless governing equations for the MHD channel flow are given by

$$\frac{\partial\mathbf{v}}{\partial t}=\frac{1}{\mathrm{Re}}\nabla^2\mathbf{v}-\nabla P-(\mathbf{v}\cdot\nabla)\mathbf{v}-\mathrm{N}(\mathbf{j}\times\mathbf{B}),$$
$$\frac{\partial\mathbf{B}}{\partial t}=\frac{1}{\mathrm{Re_m}}\nabla^2\mathbf{B}+\nabla\times(\mathbf{v}\times\mathbf{B}),$$
$$\mathbf{j}=\frac{1}{\mathrm{Re_m}}\nabla\times\mathbf{B},$$
$$\nabla\cdot\mathbf{v}=0,\qquad \nabla\cdot\mathbf{B}=0.$$

The characteristic numbers, including Reynolds number, magnetic Reynolds number, Stuart number and Hartmann number are defined as:

$$\mathrm{Re}=\frac{U_0L}{\nu},\quad \mathrm{Re_m}=\mu\sigma U_0L,\quad \mathrm{N}=\frac{\sigma B_0^2L}{\rho U_0},\quad \mathrm{Ha}=\sqrt{\mathrm{NRe}}.$$

The Hartmann number is used to indicate the interaction level between the magnetic field and the velocity field. The physical properties of the fluid, including the mass density ρ, the dynamic viscosity ν, the electrical conductivity σ and the magnetic permeability μ, are all assumed constant.

In this paper, we consider MHD flows at low magnetic Reynolds numbers ($\mathrm{Re_m}\ll 1$), which are also called simplified MHD (SMHD) flows. In these flows the induced magnetic field is negligible in comparison with the imposed magnetic field. The 3D SMHD channel flow is described by slightly modified incompressible Navier-Stokes (N-S) equations and a Poisson's equation for the electric potential:

$$\frac{\partial\mathbf{v}}{\partial t}+(\mathbf{v}\cdot\nabla)\mathbf{v}=-\nabla p+\frac{1}{\mathrm{Re}}\nabla^2\mathbf{v}+\mathrm{N}\left[(-\nabla\varphi+\mathbf{v}\times\mathbf{B_0})\times\mathbf{B_0}\right], \quad (1)$$
$$\nabla^2\varphi=\nabla\cdot(\mathbf{v}\times\mathbf{B_0})=\mathbf{B_0}\cdot\omega, \quad (2)$$
$$\nabla\cdot\mathbf{v}=0, \quad (3)$$

where $\omega=\nabla\times\mathbf{v}$ is the vorticity, $\mathbf{B_0}=\hat{\mathbf{y}}$ is the imposed magnetic field (which is simply a unit vector due to the non-dimensionalization). A detailed derivation can be found in [15]. The boundary conditions are given by

$$\mathbf{v}(x,\pm1,t)=\mathbf{0},\qquad \varphi(x,-1,t)=\varphi_b,\qquad \varphi(x,1,t)=\varphi_p,$$

where φ_b and φ_p are determined by the controller.

The N-S equation for channel flows can be written in terms of the wall-normal velocity v and the wall-normal component of the vorticity η. The other components of the velocity can be recovered by (3) and the definition of the wall-normal vorticity ($\eta=\partial_z u-\partial_x w$). Following a procedure similar to the derivation of the Orr-Sommerfeld and Squire equations, we can write the linearized SMHD equations as follows:

$$\left[\left(\frac{\partial}{\partial t}+U\frac{\partial}{\partial x}\right)\Delta-U''\frac{\partial}{\partial x}-\frac{1}{\mathrm{Re}}\Delta^2+\mathrm{N}\frac{\partial^2}{\partial y^2}\right]v=0,$$
$$\left(\frac{\partial}{\partial t}+U\frac{\partial}{\partial x}-\frac{1}{\mathrm{Re}}\Delta+\mathrm{N}\right)\eta=-U'\frac{\partial v}{\partial z}+\mathrm{N}\left(\frac{\partial^2\varphi}{\partial x^2}+\frac{\partial^2\varphi}{\partial z^2}\right),$$
$$\Delta\varphi=\eta.$$

where $\Delta=\nabla^2=\left(D^2-k_0^2\right)$ is the Laplacian operator and D is the first derivative operator in the y direction.

By computing the Fourier transforms in the x and z directions, the system above can be divided into a series of independent ODE systems, each representing the evolution of a particular wave number pair $\{k_x,k_z\}$ (see, for example, [16], for more details):

$$\Delta\dot{v}=\left[\frac{1}{\mathrm{Re}}\Delta^2-ik_xU\Delta+ik_xU''+\mathrm{N}D^2\right]v, \quad (4)$$
$$\dot{\eta}=\left[-ik_zU'\right]v+\left[\frac{1}{\mathrm{Re}}\Delta-ik_xU-\mathrm{N}\right]\eta+\left[\mathrm{N}k_0^2\right]\varphi. \quad (5)$$

Note that both v and η have been transformed into Fourier space (whether the variables are either in physical space or Fourier space can be determined by the context). In order to write the system in a standard state-space form, the operator D^2 is discretized by the Chebyshev collocation. The Laplacian operator can be inverted if appropriate boundary conditions are given when constructing the D^2 operator matrix. This is done by using the Differentiation Matrix Suite developed by Weideman & Reddy [17]. The Poisson's equation for the electric potential can also be inverted in a similar manner.

The output of the system is selected as the boundary vorticity flux, defined as.

$$\sigma = (\sigma_b, \sigma_p)^T = \left(\left.\frac{\partial \eta}{\partial y}\right|_{y=-1}, \left.\frac{\partial \eta}{\partial y}\right|_{y=1} \right)^T.$$

The physical viability and numerical convenience leads to this selection. From a physical perspective, we know that although the boundary vorticity flux can not be measured directly it can be determined by boundary pressure gradients, which can be measured [18]. From a numerical perspective, it is straightforward to calculate the vorticity flux by taking the first derivative of the vorticity at the boundaries. Then, the equations can be further written as

$$\dot{v} = M_{vv} v, \tag{6}$$
$$\dot{\eta} = M_{v\eta} v + M_{\eta\eta}\eta + M_{\varphi\eta}\varphi, \tag{7}$$
$$\varphi = M_{\eta\varphi}\eta + M_{\theta\varphi}\theta, \tag{8}$$
$$\sigma = M_{\eta\sigma}\eta, \tag{9}$$

where $\theta = (\varphi_b, \varphi_p)^T$ is the system input and

$$\begin{aligned}
M_{vv} &= \Delta^{-1}\left[\frac{1}{\mathrm{Re}}\Delta^2 - ik_x U\Delta + ik_x U'' + \mathrm{N}D^2\right],\\
M_{v\eta} &= -ik_z U',\\
M_{\eta\eta} &= \frac{1}{\mathrm{Re}}\Delta - ik_x U - \mathrm{N},\\
M_{\varphi\eta} &= \mathrm{N}k_0^2.
\end{aligned}$$

$M_{\eta\varphi}$ and $M_{\theta\varphi}$ are both results of the inversion of the Δ operator. $M_{\eta\sigma}$ is a part of the D operator that computes the first derivatives at the boundaries.

A standard state-space model G_0 can be finally written as

$$\begin{aligned}
\dot{\xi} &= A\xi + B\theta,\\
\sigma &= C\xi,
\end{aligned}$$

where $\xi = (v, \eta)^T$ and

$$A = \begin{bmatrix} M_{vv} & 0 \\ M_{v\eta} & M_{\eta\eta} + M_{\varphi\eta}M_{\eta\varphi} \end{bmatrix}, \quad B = \begin{bmatrix} 0 \\ M_{\varphi\eta}M_{\theta\varphi} \end{bmatrix},$$
$$C = \begin{bmatrix} 0 & M_{\eta\sigma} \end{bmatrix}.$$

This LSMHD system model serves as the basis for the controller design.

III. Controller Design

The LSMHD system is constructed by performing a discretization in the y coordinate on a grid of 64 Chebyshev collocation points in order to form a set of linear ODE's. The resulting system is then analyzed by modern control techniques. The system dynamics consists of two major parts: velocity v and vorticity η. The velocity equation (6) closely resembles the Orr-Sommerfeld equation, while the vorticity equation (7) resembles the Squire equation. They differ only by two extra terms produced by the Lorentz force. Like the Orr-Sommerfeld/Squire system, the velocity equation has its independent dynamics and the vorticity equation is driven by the velocity. The original Orr-Sommerfeld equation has a critical Reynolds number ($\mathrm{Re} \approx 5772$), where the equation turns linearly unstable [16], [19]. The extra Lorentz force terms tends however to stabilize the system, as indicated by the movement of eigenvalues towards the left-half complex plane when magnetic fields are imposed (Table I).

TABLE I
Six most significant eigenvalues ($\mathrm{Re} = 6500$, $k_x = 1$, $k_z = 0$)

Ha = 0	Ha = 0.8	Ha = 2.5
$0.0011 \pm 0.256i$	$-0.0026 \pm 0.255i$	$-0.0075 \pm 0.912i$
$-0.0089 \pm 0.991i$	$-0.0087 \pm 0.981i$	$-0.0209 \pm 0.899i$
$-0.0265 \pm 0.973i$	$-0.0258 \pm 0.964i$	$-0.0289 \pm 0.249i$
$-0.0436 \pm 0.956i$	$-0.0423 \pm 0.947i$	$-0.0333 \pm 0.886i$
$-0.0436 \pm 0.956i$	$-0.0423 \pm 0.947i$	$-0.0338 \pm 0.887i$
$-0.0440 \pm 0.956i$	$-0.0428 \pm 0.947i$	$-0.0344 \pm 0.886i$

The objective of our controller is indeed to destabilize the system so that it becomes linearly unstable when an imposed magnetic field is present. First, we perform an H^∞ normalized coprime factor controller synthesis to generate a stabilizing controller. The H^∞ synthesis is done upon an already stable system ($\mathrm{Re} = 6500$, $k_x = 1$, $k_z = 0$, $\mathrm{Ha} = 2.5$). The result of the H^∞ synthesis has the same order as the original system G_0. To simplify the implementation of the controller in the numerical simulator, model reduction is carried out to represent the controller as a second-order system. Next, the sign of the resulting controller is reversed in order to destabilize the closed-loop system with positive feedback. The reversed controller K takes a standard state-space form

$$\begin{aligned}
\dot{x} &= A_K x + B_K \sigma,\\
\theta &= C_K x + D_K \sigma.
\end{aligned}$$

Finally, a saturation limit is imposed on the actuator to ensure the system remains bounded.

TABLE II
Most significant eigenvalues ($\mathrm{Re} = 6500$, $k_x = 1$, $k_z = 0$)

	Ha = 0.8	Ha = 2.5
Open loop	$-0.0026 \pm 0.255i$	$-0.0075 \pm 0.912i$
Closed loop	$0.0149 \pm 0.116i$	$0.2953 \pm 0.083i$

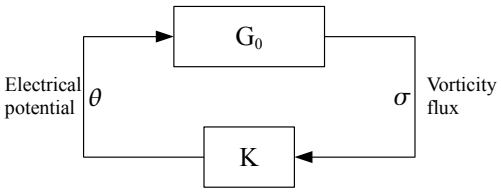

Fig. 2. Feedback loop overview

A simple closed-loop architecture based on this controller, as illustrated in Fig. 2, can be linearly unstable. This can be seen from Table II where both stable systems in Table I become linearly unstable under the effect of the controller K. Although the controller is designed to excite the $k_x=1$, $k_z=0$ mode, it is also effective in exciting higher order modes, which is necessary to achieve the desired turbulence level. Therefore, in the simulation results presented in the following section all the Fourier modes are excited using the same controller K and the same saturation limit.

IV. Simulation Results

The numerical simulations are carried out by a modified Navier-Stokes solver, originally written by T. Bewley [20]. The equations are discretized using FFT in the x and z directions and finite differences in the y direction, which is also called the pseudospectral method. Time integration is done using a fractional step method along with a hybrid Runge-Kutta/Crank-Nicolson scheme. Linear terms are treated implicitly by the Crank-Nicolson method and nonlinear terms are treated explicitly by the Runge-Kutta method. The divergence-free condition is fulfilled by the fractional step method. The controller is implemented as a second order time-evolving system using fully implicit time integration. All the simulations are carried out for the same flow domain: $0<x<d=2\pi$, $0<z<\pi$ and $0<y<1$. The same mesh is used in all the simulations presented in this section (same number of grid points in all directions: NX=NY=NY=64).

A. MHD flows with no control

When Ha=0, the SMHD system reduces to the well-known Navier-Stokes equation. The three-dimensional channel flow, which is also known as the plane Poiseuille flow, is frequently cited as a paradigm for transition to turbulence, and has drawn extensive attention through the history of fluid dynamics. This is a classical flow control problem that has been studied in [4] and the references therein assuming the availability of an array of pressure sensors on the walls and an array of MEM micro-jet actuators (also distributed along the walls) capable of blowing/suction. Incompressible conventional flows in 3D channels can be linearly stable for low Reynolds numbers, as infinitesimal perturbations in the flow field are damped out. The flows turn linearly unstable for high Reynolds numbers. Such flows usually reach statistically steady states, which we call fully established flows. An initial equilibrium velocity profile is infinitesimally perturbed at $t=0$ and Fig. 3(a) shows the flow (Re=6500) in its fully established state. In the figure the horizontal direction is x and the vertical direction is y.

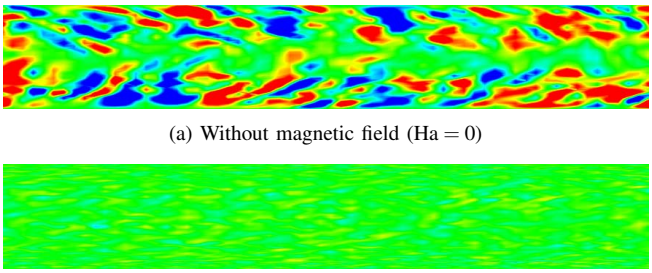

(a) Without magnetic field (Ha = 0)

(b) With imposed magnetic field imposed (Ha = 2.5)

Fig. 3. Vorticity maps of uncontrolled flows ($z=1.03$)

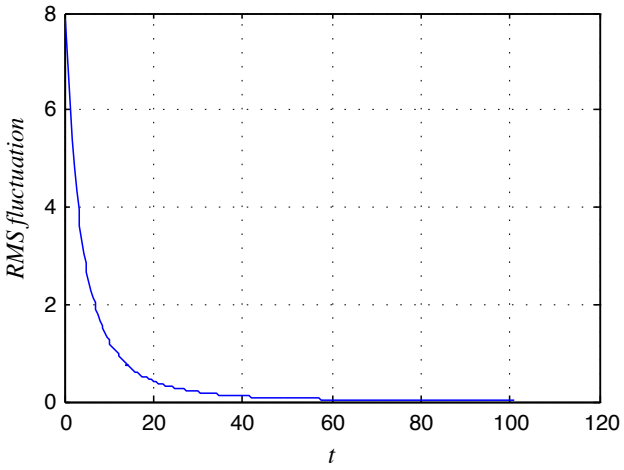

Fig. 4. RMS fluctuation of the uncontrolled flow

When Ha$\neq$0, Fig. 3(b) shows the effect of the imposed transverse magnetic field on the stability properties of the flow. Vorticity maps obtained through direct numerical simulation studies show the stabilizing effect of the imposed magnetic field on the 3D Hartmann flow. The simulation is started at $t=0$ with the fully established flow achieved in Fig. 3(a) and an imposed magnetic field (Ha = 2.5). The RMS fluctuation is often used as an indicator of turbulence, which is defined as

$$\frac{1}{\pi}\frac{1}{2\pi}\left[\int_0^{\pi}\int_0^{1}\int_0^{2\pi}(\mathbf{v}(x,y,z,t)-\bar{\mathbf{v}}(y,t))^2\,dxdydz\right]^{\frac{1}{2}}, \quad (10)$$

where

$$\bar{\mathbf{v}}(y,t)=\frac{1}{\pi}\frac{1}{2\pi}\int_0^{\pi}\int_0^{2\pi}\mathbf{v}(x,y,z,t)dxdy. \quad (11)$$

A completely laminar flow would give a zero RMS fluctuation because of the lack of velocity components in the x and z directions. Fig. 4 confirms that the perturbation is effectively damped out by the MHD effects as the RMS gradually decreases towards zero.

B. MHD flows with boundary feedback control by electric potential

In this section, the feedback boundary controller K based on the LSMHD model is tested. All the simulations start

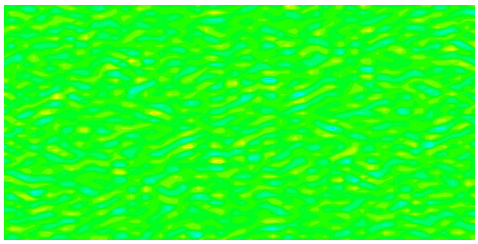

(a) $t = 0.016$

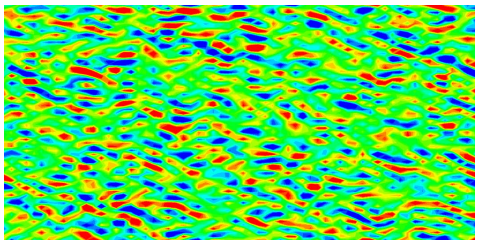

(b) $t = 0.3$

Fig. 5. Vorticity development ($y = 0.0837$)

with equilibrium solutions achieved after an external magnetic field is imposed. Simulations are conducted for these parameters:

$$\mathrm{Re} = 6500, \qquad Q = 1.5, \qquad \mathrm{Ha} = 2.5,$$

and the saturation limit on the output of K is set to 0.05. The flow remains linearly stable indefinitely if no boundary control is present. The boundary control is expected to drive the flow to states with higher RMS fluctuation levels, thus enhancing mixing.

Fig. 5 shows two snapshots of vorticity maps η at a fixed y plane at different time instances of the simulation. In the figures the horizontal direction is x and the vertical direction is z. We can clearly see that the vorticity is significantly enhanced and complex flow structures occur due to the boundary control. At a very early stage of the simulation, the effect of the controller can already be seen in Fig. 5(a) as the small perturbation is introduced by the rapidly growing electric potential actuators. The controller soon reaches saturation on all of the excited modes.

The growth of the vortices, however, does not stop after the controller is saturated. This can be seen in the development of Reynolds stresses in Fig. 6, which shows the averaged (over the x and z coordinates) profile of one of the Reynolds stresses, R_{uw}, in the lower half channel at three different time instances. The maximum Reynolds stress occurs very close to the boundary, which indicates that the penetration of the flow structures is somehow limited to the boundary regions. This is, however, expected because the main effect of the controller is on the wall-normal vorticity $\eta = \partial_x u - \partial_x w$, which does not involve the wall-normal velocity v. The relation of (6) and (7) determines that the wall-normal velocity is not directly controllable in the LSMHD model. The controller has to rely on the nonlinear interaction of the wall-normal vorticity to generate wall-normal velocity. The lack of direct control over wall-normal velocity limits the penetration of the

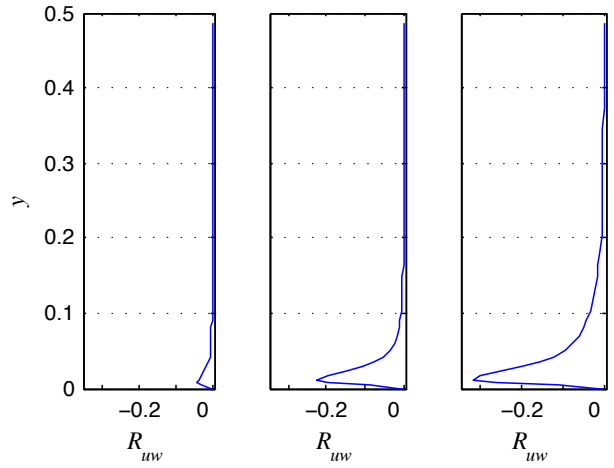

Fig. 6. R_{uw} profiles ($t = 0.08$, 0.24, 2)

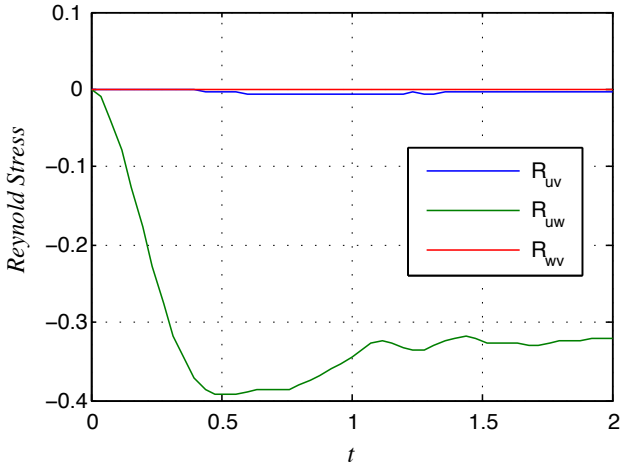

Fig. 7. Reynolds stress development ($y = 0.0122$)

vortices. Fig. 7 shows all three Reynolds stresses averaged over the x and z coordinates at the $y = 0.0122$ plane, where the peak of Reynolds stress occurs. The domination by the R_{uw} component confirms that the controller is efficient in controlling the wall-normal vorticity, and has very limited contribution to the wall-normal velocity.

The wall-normal velocity and vorticity contour maps of a statistically steady state at a certain z plane is given by Fig. 8. In the maps the horizontal direction is x and the vertical direction is y. We can see that the controller is highly effective in the generation of intense wall-normal vorticity near the boundaries, while the wall-normal velocity is relatively small because of the lack of direct actuation. It is evident that a means to enhance the transportation along the wall-normal direction is necessary.

The actuation of the controller is visualized by the potential contour on a y plane very close to the boundary, as the electric potential is almost identical to the one on the boundary. As Fig. 9 shows, the controller has a very rich frequency content, due to the excitation of all Fourier modes. The RMS fluctuation development (Fig. 10) clearly

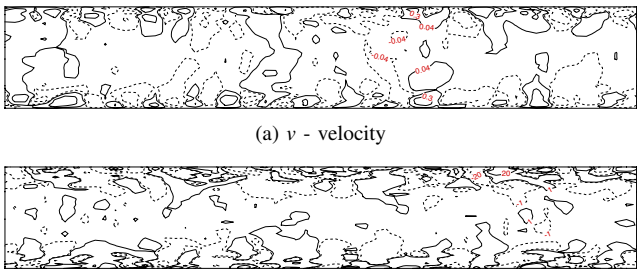

(a) v - velocity

(b) η - vorticity

Fig. 8. Wall-normal velocity and vorticity ($t = 2$, $z = 1.03$)

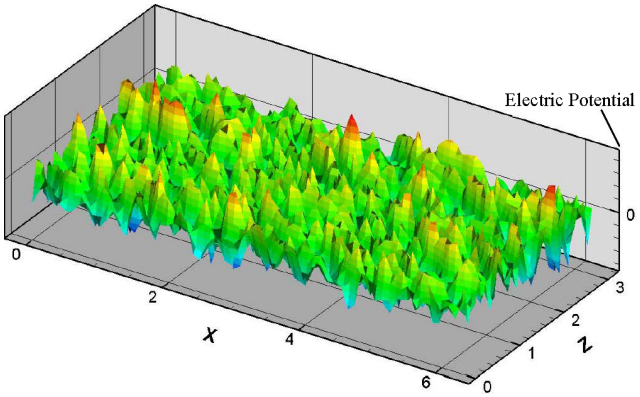

Fig. 9. Electric potential contour on an x-z plane ($t = 0.3$, $y = 0.00837$)

shows that the overall turbulence level of an initially stable MHD flow is increased by the feedback control to a level 4.6 times higher than that corresponding to an uncontrolled fully developed pure hydrodynamic flow (characterized by the initial RMS fluctuation value in Fig. 4).

V. Conclusion

We propose a boundary controller based on electric potential actuation for mixing enhancement in a 3D MHD channel flow. The controller is based on a linearized SMHD model which is discretized by spectral methods. Simultaneous excitation of all the modes is crucial for the success of the controller. A simple second-order feedback control is proved to be able to destabilize the vorticity field. A simple saturation limit is imposed on the actuator to bound the growth driven by the destabilizing controller. In this way the system can remain turbulent and bounded. The 3D SMHD simulation study confirms the effectiveness of the controller by showing increases in the RMS fluctuation and Reynolds stress levels of the otherwise linearly stable flow, thus increasing mixing effects inside the channel. The simulation also reveals that the wall-normal penetration of the generated turbulence is limited.

Future work includes further study of the destabilizing mechanism of the controller with the ultimate goal of enhancing wall-normal penetration. The simultaneous control of wall-normal vorticity using electric potential actuation and of wall-normal velocity using mechanical actuation (blowing and suction) appears as promising.

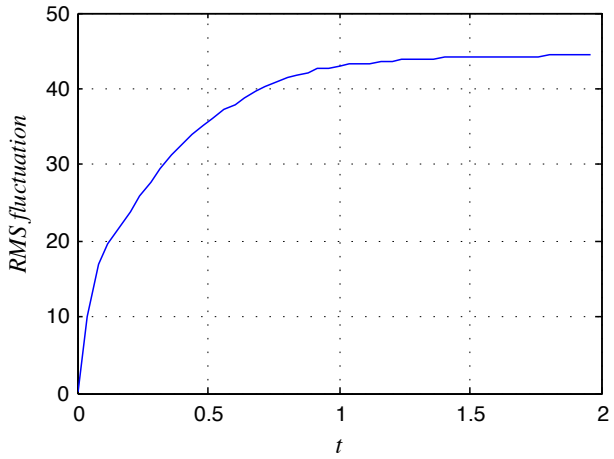

Fig. 10. RMS fluctuation of controlled flow

References

[1] U. Müller and L. Bühler, *Magnetofluiddynamics in Channels and Containers*. Springer, 2001.

[2] M. D. Gunzburger, *Flow Control*, ser. The IMA Volumes in Mathematics and its Applications. New York: Springer-Verlag, 1995, vol. 68.

[3] S. S. Sritharan, Ed., *Optimal Control of Viscous Flow*. SIAM, Philadelphia, 1998.

[4] O. M. Aamo and M. Krstić, *Flow Control by Feedback*. Springer, 2002.

[5] M. R. Jovanovic, "Turbulence suppression in channel flows by small amplitude transverse wall oscillations," *Physics of Fluids*, vol. 20, no. 1, p. 014101, 2008.

[6] A. B. Tsinober, *Viscous Drag Reduction in Boundary Layers*, ser. Progress in Astronautics and Aeronautics. Washington, DC: AIAA, 1990, no. 123, ch. MHD flow drag reduction, pp. 327–349.

[7] H. Choi, P. Moin, and J. Kim, "Active turbulence control for drag reduction in wall-bounded flows," *J.Fluid Mech.*, vol. 262, p. 75, 1994.

[8] C. Henoch and J. Stace, "Experimental investigation of a salt water turbulent boundary layer modified by an applied streamwise magnetohydrodynamic body force," *Physics of Fluids*, vol. 7, no. 6, pp. 1371–1383, June 1995.

[9] T. Berger, J. Kim, C. Lee, and J. Lim, "Turbulent boundary layer control utilizing the Lorentz force," *Physics of Fluids*, vol. 12, p. 631, 2000.

[10] E. Spong, J. Reizes, and E. Leonardi, "Efficiency improvements of electromagnetic flow control," *Heat and Fluid Flow*, vol. 26, pp. 635–655, 2005.

[11] E. Schuster, L. Luo, and M. Krstić, "MHD channel flow control in 2D: Mixing enhancement by boundary feedback," *Automatica*, vol. 44, no. 10, pp. 2498–2507, 2008.

[12] L. Luo and E. Schuster, "Heat transfer enhancement in 2D magnetohydrodynamic channel flow by boundary feedback control," in *Proceedings of 45th IEEE Conference on Decision and Control*, San Diego, 2006, pp. 5317–5322.

[13] ——, "Boundary feedback control for heat exchange enhancement in 2D magnetohydrodynamic channel flow by extremum seeking," in *Proceedings of the 48th IEEE Conference on Decision and Control*, Shanghai, China, December 2009.

[14] J. Hartmann, *Theory of the Laminar Flow of an Electrically Conductive Liquid in a Homogeneous Magnetic Field*, xv(6) ed. Det Kgl. Danske Vidensk-abernes Selskab Mathematisk-fysiske Meddelelser.

[15] G. Branover, *Magnetohydrodynamic Flow in Ducts*. Halsted Press, 1979.

[16] P. J. Schmid and D. S. Henningson, *Stability and Transition in Shear Flows*. New York: Springer, 2001, vol. 142.

[17] J. A. C. Weideman and S. C. Reddy, "A MATLAB differentiation matrix suite," *ACM Transactions on Mathematical Software*, vol. 26, no. 4, pp. 465–519, December 2000.

[18] G. H. Cottet and P. D. Koumoutsakos, *Vortex Methods: Theory and Practice*. Cambridge university press, 2000.

[19] R. L. Panton, *Incompressible flow*, 2nd ed. New York: Wiley, 1996.

[20] T. R. Bewley, *Optimal and Robust Control and Estimation of Transition, Convection, and Turbulence*. Stanford University thesis, 1999.